First-Principles Modeling of the Polycyclic Aromatic Hydrocarbons Reduction

ARTICLE *in* THE JOURNAL OF PHYSICAL CHEMISTRY C · JULY 2011

Impact Factor: 4.77 · DOI: 10.1021/jp2024928 · Source: arXiv

3 AUTHORS, INCLUDING:

D. W. Boukhvalov
Hanyang University
101 PUBLICATIONS **4,167** CITATIONS
SEE PROFILE

Xumeng Feng
Nanjing Agricultural University
79 PUBLICATIONS **738** CITATIONS
SEE PROFILE

THE JOURNAL OF PHYSICAL CHEMISTRY C

ARTICLE

pubs.acs.org/JPCC

First-Principles Modeling of the Polycyclic Aromatic Hydrocarbons Reduction

D. W. Boukhvalov,*[,†] X. Feng,[‡] and K. Müllen[‡]

[†]School of Computational Sciences, Korea Institute for Advanced Study (KIAS), Hoegiro 87, Dongdaemun-Gu, Seoul, 130-722, Korean Republic

[‡]Max Planck Institute for Polymer Research, Ackermannweg 10, 55128 Mainz, Germany

ABSTRACT: Density functional theory modeling of the reduction of realistic nanographene molecules ($C_{42}H_{18}$, $C_{48}H_{18}$, and $C_{60}H_{24}$) by molecular hydrogen evidence of the presence of limits in the hydrogenation process. These limits caused the contentions between three-fold symmetry of polycyclic aromatic hydrocarbon molecules and two-fold symmetry of adsorbed hydrogen pairs. Increase in the binding energy between nanographenes during reduction is also discussed as a possible cause of the experimentally observed limited hydrogenation of studied nanographenes.

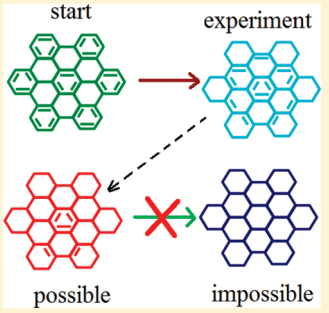

1. INTRODUCTION

Hydrogenation of aromatic hydrocarbons and related carbon materials is an actual topic in modern experimental (ref 1 and references therein) and computational[2,3] chemistry. Fabrication of the hydrogenated graphene monolayer, namely, graphane,[4] has stimulated the interests for the functionalization of the nanographenes. Further experimental results[5] suggest the significant sample dependency of the hydrogenation processes of graphene.[4] Previous calculations[2,6] discuss the leading role of the edges for the hydrogenation process of graphene nanoribbons. The similarity of the atomic structure between graphene[7] and polycyclic aromatic hydrocarbons (PAHs)[8,9] suggests that defined PAH could be a suitable model for the modeling of graphene hydrogenation. Theoretical prediction of the intriguing electronic and magnetic properties of the graphene and graphene nanoribbons,[10] nanoengineering of graphene by partial hydrogenation,[11] manufacturing of several graphenic nanoribbons from PAHs,[9] and experimentally detected limits in PAH reduction by catalytic hydrogenation[1] also require detailed survey of the hydrogenation of PAH with given shape.

The previous works[12−14] suggest that density functional theory (DFT) is the powerful tool for the modeling of realistic chemistry of compounds with a honeycomb lattice.[4] In the present work, we studied step-by-step reduction of hexa-*peri*-hexabenzocoronene (HBC, $C_{42}H_{18}$ **1**, the structure is shown in Figure 1) and two other graphene molecules with different shapes ($C_{48}H_{18}$ **2** and $C_{60}H_{24}$ **3**, shown in Figures 2 and 3, respectively). To check the possibility of stack formation between partially hydrogenated PAH molecules in the process of hydrogenation calculation of the binding energies for the initial, we have performed intermediate and final studies of functionalization.

2. COMPUTATIONAL METHOD AND MODEL

The modeling was carried out by DFT realized in the pseudopotential code SIESTA,[15] as was done in our previous works.[4,12,16] For the hydrogenation processes, all calculations were done using the generalized gradient approximation (GGA-PBE),[17] which is the most suitable for the description of graphene-adatom chemical bonds.[4,6,12] Full optimization of all atomic positions was performed. During the optimization, the electronic ground state was found self-consistently using norm-conserving pseudopotentials for cores and a double-ζ plus polarization basis of localized orbitals for carbon and oxygen and double-ζ basis for hydrogen. Optimization of the forces and total energies was performed with an accuracy of 0.04 eV/Å and 1 meV, respectively. All calculations were carried out for an energy mesh cutoff of 360 Ry and a *k*-point mesh 8 × 8 × 1 in the Mokhorst−Pack scheme.[17] All calculations have been performed in spin-polarized mode. Use of this mode for the knowingly nonmagnetic configurations is the important issue of the modeling of graphene and related systems functionalization. Incorrect initial structures should provide magnetic configurations after several loops of the self-consistent process. Calculations in this mode could help the computational time usually spent due to very probable misprints in the starting configurations.

Received: March 16, 2011
Revised: July 7, 2011
Published: July 08, 2011

dx.doi.org/10.1021/jp2024928 | *J. Phys. Chem. C* 2011, 115, 16001–16005

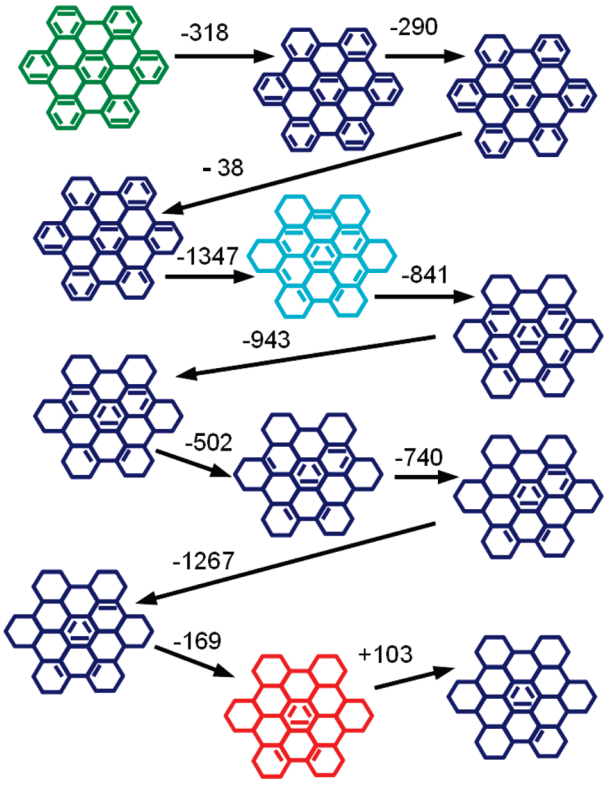

Figure 1. Sketch of step-by-step reduction of hexabenzocoronene ($C_{42}H_{18}$, **1**). All energies are shown in meV/H_2. The initial structure is indicated by green, the intermediate stable structure obtained in the experiment[1] (see description in text) is indicated by cyan, and the final structure is indicated by red.

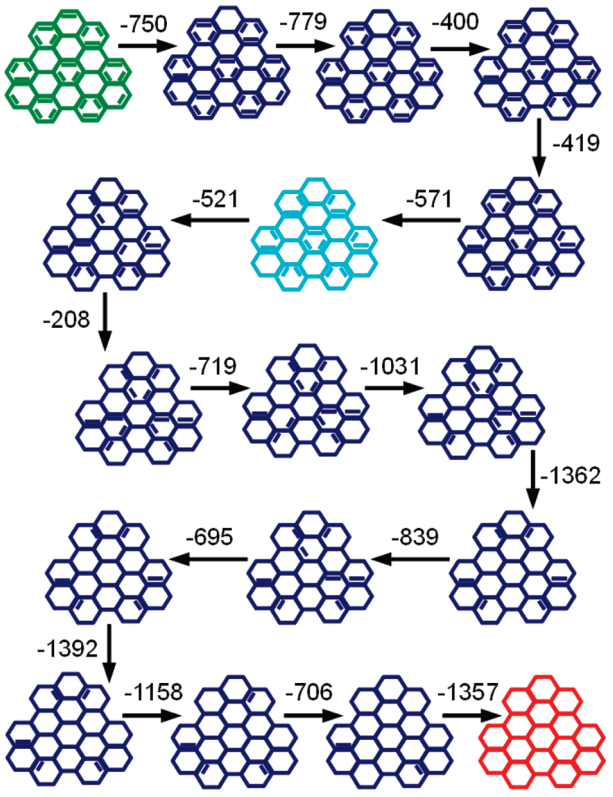

Figure 2. Sketch of step-by-step reduction of $C_{48}H_{18}$ (**2**). All energies are shown in meV/H_2. The initial structure is indicated by green, the intermediate stable structure (see description in text) is indicated by cyan, and the final structure is indicated by red.

For the realistic modeling of the processes of catalytic hydrogenation by molecular hydrogen on each step of reduction process, the pair of hydrogen atoms was added from the same side on the nearest carbon atoms (ortho position) connected with a double bond. This structure is corresponding to the boatlike structure (Figure 4a). Previous calculations[17] suggest that the most energetically favorable is the chairlike structure (Figure 4b). In our modeling, we take into account possible reconstruction from boatlike to chairlike structure at the final steps of hydrogenation. The graphene molecules have been placed in the center of the empty cubic box with the side length of 4 nm. Formation energy was calculated by standard formula $E_{form} = E_{stepN+1} - (E_{stepN} - E_{H2})$, where E_{stepN} and $E_{stepN+1}$ are the total energies of the studied graphene molecules before and after chemisorption of the pair of hydrogen atoms and E_{H2} is the total energy of molecular hydrogen in empty box. Calculation of the formation energy with using the total energy of molecular hydrogen is necessary for the simulation of the realistic hydrogenation processes.

The calculations of the atomic structure and binding energies for the physisorption of benzene molecules as simplest of molecules with carbon hexagon with $\pi-\pi$ bonds on PAH with different level of hydrogenation are done using the LDA functional,[18] which is reliable for the description of graphene adsorbed molecule interaction without chemical bond formations.[16,21] The value of binding energies between graphene molecules and benzene molecules is calculated by using the standard formula $E_{bind} = E_{g+bz} - (E_g + E_{bz})$, where E_{g+bz} is the total energy of graphene molecules with adsorbed benzene molecule and E_g and E_{bz} are the total energies of graphene and benzene molecule in the same box.

3. RESULTS AND DISCUSSION

We have started the modeling of HBC from calculation of the adsorption of hydrogen pairs from one site on different sites. (See Figure 5a,b.) Similar to previous theoretical results,[2,6,12] for relevant graphitic compounds, the formation energy for hydrogenation of nanographene edges is negative, and chemisorption of the hydrogen pair in the central part is positive (~0.3 eV, near the similar value for bulk graphene[12]). For the modeling of the next steps of reduction, we have calculated the formation energies of the different probable positions of hydrogen pairs (see, for example, of the first step of hydrogenation of **1**, Figure 5c) and used the configuration with minimal total energy as starting point for the next step. It is necessary to note that for all steps of hydrogenation of all three studied compounds, the total energy of the most favorable configuration is at least 0.1 eV lower than the other. These results evidence the rather high probability of the reaction pathway reported in Figure 1.

There are two issues that seem as controversial with the experimental results[1] for the reduction of **1**. In experiments, the process of hydrogenation requires additional light heating, but all steps of the reduction reported in theory are exothermic. It is necessary to note that our model is quite ideal and exactly valid only for the gaseous phase. In contrast with realistic processes, all sites on **1** could be reached by hydrogen molecules. In experiments, the heating has been used for the transport of hydrogen

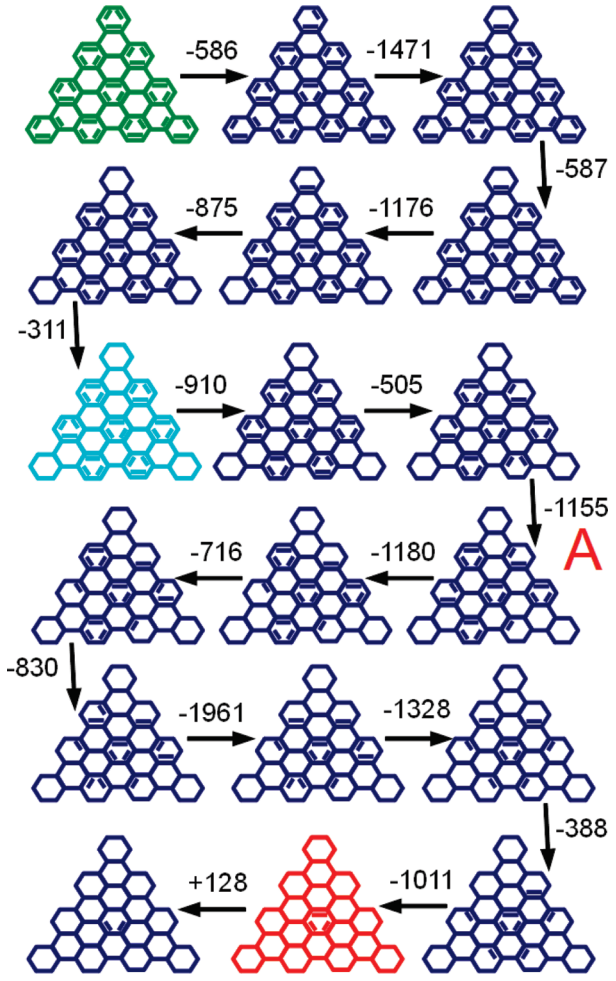

Figure 3. Sketch of step-by-step reduction of $C_{60}H_{24}$ (**3**). All energies are shown in meV/H_2. The initial structure is indicated by green, the intermediate stable structure (see description in text) is indicated by cyan, and the final structure is indicated by red. The optimized atomic structure of the configuration pointed by the letter A is shown on Figure 6.

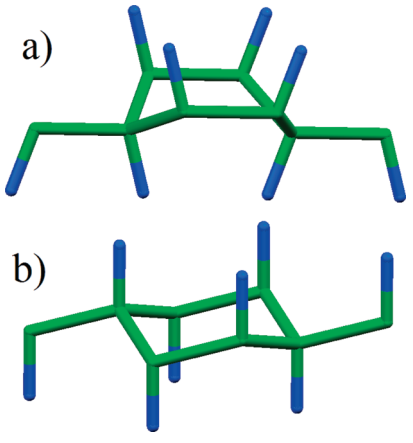

Figure 4. Optimized atomic structures of "boat" (a) and "chair" (b) atomic structures of 100% hydrogenated graphene.

molecules to the graphene surface. Therefore, the results of our calculations could be used as examination of the limits of

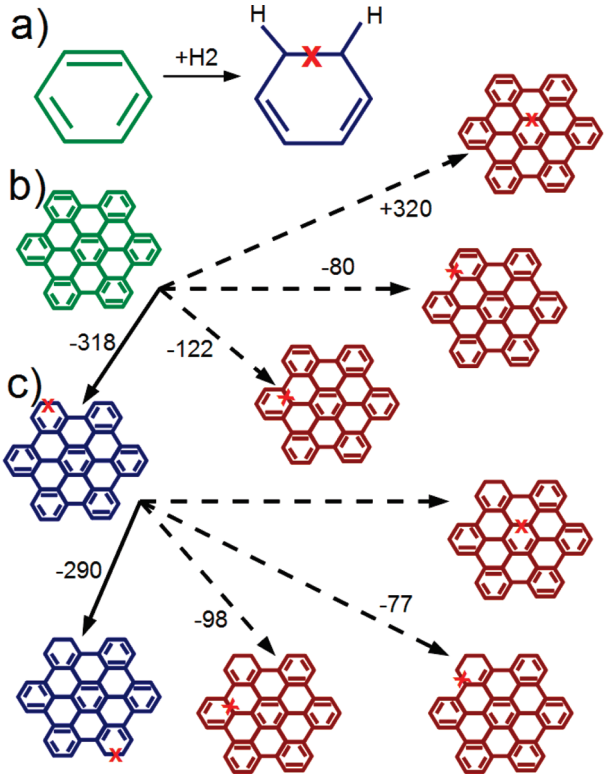

Figure 5. Sketch of the modeling of the hydrogen pair chemisorption on the carbon hexagon (a) with change of double C═C bond to single bond (shown by the red cross) and modeling process of two first steps of reduction of hexabenzocoronene ($C_{42}H_{18}$, **1**). All energies are shown in meV/H_2. Initial configurations are shown by blue, and less energetically favorable configurations are shown by brown.

reduction when exothermic processes turn to be endothermic and could be used as estimation of the temperatures required for the further steps of reduction.

Theoretical results predict a significant level of hydrogenation of **1**, but the experiment reported the reduction of only the edge peripheries. (See Figure 1.) The cause of the difference between experimental and theoretical results could be due to the changes in the binding energies between molecules of **1**. For modeling of these changes, we performed the calculation of the binding energies between studied graphene molecules at different levels of the hydrogenation and benzene molecule (minimal molecule with hexagon structure and double carbon−carbon bonds, see Figure 4). The results of calculations (Table 1) prove significant enhancement of the binding between all types of graphene molecules and benzene after hydrogenation of the edges. Further reduction leads to the increase in the binding energies. The nature of these changes of the energy of adsorption of benzene molecule on graphenes is in distortions of graphene sheet caused by hydrogenation.[6,12] The corrugations of graphene (e.g, Figure 4a,b) sheet significantly increase the binding energies between graphene and toluene[16] and should provide the formation of stack-like structures. The "conglutination" of the graphene molecules makes the central part of the molecules unachievable for the hydrogen in contrast with the planar graphene under hydrogen plasma treatment[4,5] and could be the limit of the further reduction of graphene molecules.

dx.doi.org/10.1021/jp2024928 |J. Phys. Chem. C 2011, 115, 16001–16005

Table 1. Binding Energies in meV/C_6H_6 for Adsorption of Benzene Molecules from One a Two Sides (In Parentheses) of Pure, Intermediate, and Final Level of the Reduction of 1, 2, and 3 Compounds (See Figures *1*−*3*)

compound	pure	intermediate reduction	final reduction
1	67 (87)	119 (153)	236 (312)
2	123 (122)	187 (191)	429 (497)
3	117 (123)	161 (197)	351 (379)

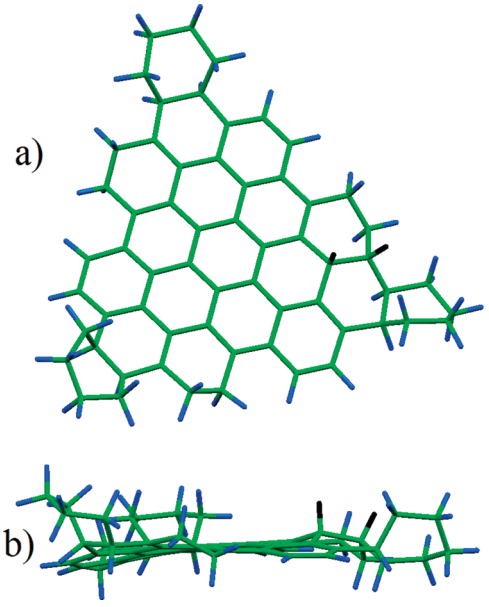

Figure 6. Optimized atomic structure of the intermediate step of the hydrogenation of PAH molecule indicated by letter A in Figure 3.

Similar to **1**, we examined the energetics of the reduction of graphene molecules **2** and **3**. For **2**, the total reduction after the exothermic step of the hydrogen adhesion is reported (Figure 2); for **3**, similarly to **1**, the significant level of the reduction could be obtained. For understanding the nature of the limit in hydrogenation due to turn exothermic to endothermic process, taking into account the symmetry of the graphene is required. In contrast with the squarelike graphenic compounds or graphene nanoribbons and nanographenes,[6] all studied molecules have six- or three-fold symmetry, but in the process of reduction, we add on each step only a pair of the hydrogen atoms. These pairs lead to local two-fold symmetry appearance. The contention between significant distortions of nanographene flat (Figure 6), local symmetry near chemisorbed pair, and symmetry of the molecule results in changes of the chemisorption energies of each step of reduction. (See Figures 1−3.) The proposed explanation works for **1** and **3**, but for the totally reducible **2**, taking into account an additional source of chemical activity is required. In contrast with **1** and **3**, the graphene molecule **2** has not only armchair but also ziz-zag edges. Larger chemical activity of this type of the graphene edges has been discussed in several theoretical works.[6,20] The presence of these types of edges in **2** enhances chemical activity of this type of graphene and leads to vanishing of the discussed above limit in the hydrogenation.

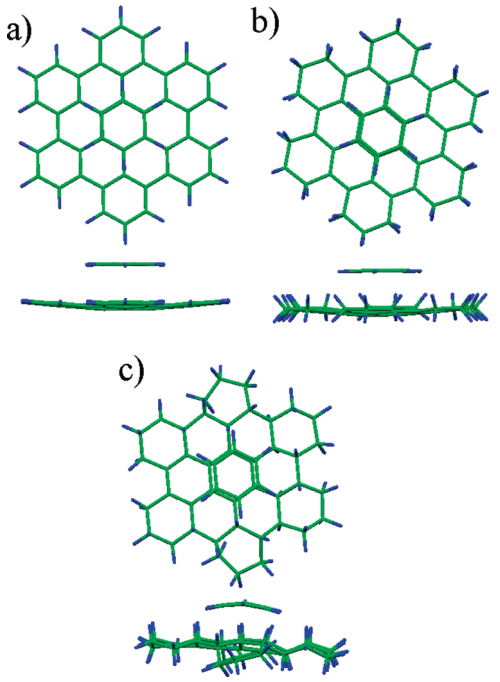

Figure 7. Optimized atomic structures of benzene molecule adsorbed on (a) pure hexabenzocoronene $C_{42}H_{18}$, (b) hexa-*peri*-hexabenzocoronene $C_{42}H_{36}$, and (c) hexabenzocoronene with maximal level of hydrogenation ($C_{42}H_{50}$).

To check the possible role of the reconstruction of the boatlike structure obtained in our calculations (Figures 4a and 6) with the most energetically favorable for graphane chairlike structure (Figure 4b), we performed calculation of the total energy for the case of the reconstruction of the obtained final configurations and find that the energy gain is ∼70 meV/H for all three structures. This result is near to that reported for the flat infinite graphene.[17] To check the influence of this reconstruction of hydrogen adatoms, we have performed the calculations for the probable next steps of reduction and found that similarly to the boatlike structure, for the chairlike structure, this processes should also be endothermic (Figures 1−3).

4. CONCLUSIONS

Performed DFT modeling of the reduction of PAHs explains the difference between hydrogenation of nanographenes and free-standing quasi-infinite graphene sheets. For the realistic nanographenes, the shape of the samples plays a crucial role. The contentions between three-fold symmetry of PAH molecules and two-fold symmetry of adsorbed hydrogen pair is the case of appearance of additional energy barriers for the total hydrogenation. Increasing of the binding energy between partially reduced nanographenes makes the central areas of these molecules unreachable for the hydrogen molecules. Taking into account these two main limitations in nanographenes functionalization is necessary for the modeling of graphene nanoribbon covalent functionalization.

AUTHOR INFORMATION

Corresponding Author

*E-mail: danil@kias.re.kr.

REFERENCES

(1) Watson, M. D.; Debije, M. G.; Warman, J. M.; Müllen, K. *J. Am. Chem. Soc.* **2004**, *126*, 766.

(2) (a) Lin, Y.; Ding, F.; Yakobson, B. I. *Phys. Rev. B* **2008**, *78*, 041402. (b) Sheka, E. F.; Chernozatonskii, L. A. *Int. J. Quantum Chem.* **2010**, *110*, 1938. (c) Sheka, E. F.; Chernozatonskii, L. A. *J. Exp. Theor. Phys.* **2010**, *110*, 121.

(3) Shahab Naghavi, S.; Gruhn, T.; Alijani, V.; Fecher, G. H.; Felser, C.; Medjanik, K.; Kutnyahov, D.; Nepijko, S. A.; Schönhense, G.; Rieger, R.; Baumgerten, M.; Müllen, K. *J. Mol. Spectrosc.,* in press.

(4) Elias, D. C.; Nair, R. R.; Mohiuddin, T. G. M.; Morozov, S. V.; Blake, P.; Halsall, M. P.; Ferrari, A. C.; Boukhvalov, D. W.; Katsnelson, M. I.; Geim, A. K.; Novoselov, K. S. *Science* **2009**, *323*, 610.

(5) Luo, Z.; Yu, T.; Kim, K.-J.; Ni, Z.; You, Y.; Lim, S.; Shen, Z.; Wang, S.; Lin, J. *ACS Nano* **2009**, *3*, 1781.

(6) (a) Boukhvalov, D. W.; Katsnelson, M. I. *Nano Lett.* **2008**, *8*, 4378. (b) Kosimov, D. P.; Dzhurakhalov, A. A.; Peeters, F. M. *Phys. Rev. B* **2010**, *81*, 195414. (c) Ao, Z. M.; Hernández-Nieves, A. D.; Peeters, F. M.; Li, S. *Appl. Phys. Lett.* **2010**, *97*, 233109.

(7) (a) Casiraghi, C.; Hartschuh, A.; Quian, H.; Piscanec, S.; Georgi, C.; Fasoli, A.; Novoselov., K. S.; Basko, D. M.; Ferrari, A. C. *Nano Lett.* **2009**, *9*, 1433. (b) Neubeck, S.; You, Y. M.; Ni, Z. H.; Blake, P.; Shen, Z. X.; Geim, A. K.; Novoselov., K. S. *Appl. Phys. Lett.* **2010**, *97*, 053110. (c) Xu, Y. N.; Zhan, D.; Liu, L.; Suo, H.; Nguyen, T. T.; Zhao, C.; Shen, Z. X. *ACS Nano*, in press.

(8) (a) Wu, J.; Pisula, W.; Müllen, K. *Chem. Rev.* **2007**, *107*, 718. (b) Riger, R.; Müllen, K. *J. Phys. Org. Chem.* **2010**, *23*, 315.

(9) (a) Cai, J.; Ruffieux, P.; Jaafar, R.; Bieri, M.; Braun, T.; Blankenburg, S.; Muoth, M.; Seitsonen, A. P.; Saleh, M.; Feng, X.; Müllen, K.; Fasel., R. *Nature* **2010**, *466*, 470. (b) Yang, X. Y.; Dou, X.; Rouhanipour, A.; Zhi, L. J.; Räder, H. J.; Müllen, K. *J. Am. Chem. Soc.* **2008**, *130*, 4216.

(10) (a) Singh, A. K.; Yakobson, B. I. *Nano Lett.* **2009**, *9*, 1540. (b) Xiang, H.; Kan, E.; Wei, S.-H.; Whangbo, M.-H.; Yang, J. *Nano Lett.* **2009**, *9*, 4025.

(11) (a) Chernozatonskii, L. A.; Sorokin, P. B. *J. Phys. Chem. C* **2010**, *114*, 3225. (b) Chernozatonskii, L. A.; Sorokin, P. B.; Bruning, J. W. *Appl. Phys. Lett.* **2007**, *91*, 183103. (c) Chernozatonskii, L. A.; Sorokin, P. B.; Belova, E. E.; Bruning, J.; Fedorov, A. S. *JETP Lett.* **2007**, *85*, 77.

(12) Boukhvalov, D. W.; Katsnelson, M. I.; Lichtenstein, A. I. *Phys. Rev. B* **2008**, *77*, 035427.

(13) Soler, J. M.; Artacho, E.; Gale, J. D.; Garsia, A.; Junquera, J.; Orejon, P.; Sanchez-Portal, D. *J. Phys.: Condens. Matter* **2002**, *14*, 2745.

(14) Boukhvalov, D. W *Surf. Sci.* **2010**, *604*, 2190.

(15) Perdew, J. P.; Burke, K.; Ernzerhof, M. *Phys. Rev. Lett.* **1996**, *77*, 3865.

(16) Monkhorst, H. J.; Park, J. D. *Phys. Rev. B* **1976**, *13*, 5188–92.

(17) Sofo, J. O.; Chaudhari, A. S.; Barber, G. D. *Phys. Rev. B* **2007**, *75*, 153401.

(18) Perdew, J. P.; Zunger, A. *Phys. Rev. B* **1981**, *23*, 5048.

(19) (a) Ataca, C.; Aktürk, E.; Ciraci, S. *Phys. Rev. B* **2009**, *79*, 041406. (b) Ataca, C.; Aktürk, E.; Ciraci, S.; Ustunel, H. *Appl. Phys. Lett.* **2008**, *93*, 043123. (c) Ao, Z. M.; Peeters, F. M. *Phys. Rev. B* **2010**, *81*, 205406. (d) Leenaerts, O.; Partoens, B.; Peeters, F. M. *Phys. Rev. B* **2009**, *79*, 2235440. (e) Leenaerts, O.; Partoens, B.; Peeters, F. M. *Microelectron. J.* **2009**, *40*, 860. (f) Leenaerts, O.; Partoens, B.; Peeters, F. M. *Appl. Phys. Lett.* **2008**, *92*, 243125. (g) Leenaerts, O.; Partoens, B.; Peeters, F. M. *Phys. Rev. B* **2008**, *77*, 125416. (h) Wehling, T. O.; Novoselov, K. S.; Morozov, S. V.; Vdovin, E. E.; Katsnelson, M. I.; Geim, A. K.; Lichtenstein, A. I. *Nano Lett.* **2008**, *8*, 173. (i) Wehling, T. O.; Katsnelson, M. I.; Lichtenstein, A. I. *Appl. Phys. Lett.* **2009**, *93*, 202110. (j) Ribeiro, R. M.; Peres, N. M. R.; Coutinho, J.; Briddon, P. R. *Phys. Rev. B* **2008**, *78*, 075442. (k) Zanella, I.; Guerini, S.; Fagan, S. B.; Mendes Filho, J.; Souza Filho, A. G. *Phys. Rev. B* **2008**, *77*, 073404. (l) Cordero, N. A.; Alonso, J. A. *Nanotechnology* **2007**, *18*, 485705. (m) Widenkvist, E.; Boukhvalov, D. W.; Rubino, S.; Akhtar, S.; Lu, J.; Quinlan, R. A.; Katsnelson, M. I.; Leefer, K.; Grennberg, H.; Jansson, U. *J. Phys. D: Appl. Phys.* **2009**, *42*, 112003.

(20) Rouhanipour, A.; Roy, M.; Feng, X.; Räder, H. J.; Müllen, K. *Angew. Chem., Int. Ed.* **2009**, *48*, 4602.

(21) (a) Yang, S. B.; Feng, X.; Wang, L.; Tang, K.; Maier, J.; Müllen, K. *Angew. Chem., Int. Ed.* **2010**, *49*, 4795. (b) Räder, H. J.; Rouhanipour, A.; Talarico, A. M.; Palermo, V.; Samorì, P.; Müllen, K. *Nat. Mater.* **2006**, *5*, 276. (c) Laursen, B. W.; Norgaard, K.; Reitzel, N.; Simonsen, J. B.; Nielsen, C. B.; Als-Nielsen, J.; Bjornholm, T.; Solling, T. I.; Nielsen, M. M.; Bunk, O.; Kjaer, K.; Tchebotareva, N.; Watson, M. D.; Müllen, K.; Piris, J. *Langmuir* **2004**, *20*, 4139.